Journal Name

RSCPublishing

ARTICLE

Cite this: DOI: 10.1039/x0xx00000x

Received 00th January 2012,
Accepted 00th January 2012

DOI: 10.1039/x0xx00000x

www.rsc.org/

Highly luminescent nitrogen-doped carbon quantum dots as effective fluorescent probes for mercuric and iodide ions†

Zi Li,[a,b,‡] Huijun Yu,[b,c,‡] Tong Bian,[b] Yufei Zhao,[b] Chao Zhou,[b] Lu Shang,[b] Yanhui Liu,[a] Li-Zhu Wu,[b] Chen-Ho Tung[b] and Tierui Zhang*[b]

Nitrogen-doped carbon quantum dots (N-CQDs) with strong blue fluorescence and high quantum yield of 66.8% were synthesized via a facile one-pot hydrothermal treatment with ammonium citrate and ethylenediamine as carbon and nitrogen sources, respectively. The blue fluorescence emission is independent of the excitation wavelengths and is very stable in a wide pH range. These N-CQDs, well dispersed in water and other polar solvents, showed a highly selective and sensitive detection of hazardous and toxic Hg^{2+} in the range of 10 nM - 20 μM through a fluorescence quenching process. The quenched N-CQDs by Hg^{2+} exhibited high selectivity and sensitivity for I^- in the range of 0.5 μM - 40 μM via a fluorescence recovery process. A possible charge transfer process responsible for the effective detections was proposed according to the UV-Vis absorption and fluorescence decay measurements.

Introduction

In recent years, great attentions have been paid to carbon quantum dots (CQDs) in the field of bioimaging,[1-4] medical diagnosis,[5-7] catalysis,[8-10] and photovoltaic devices[11, 12] due to their unique properties, such as size-dependent photoluminescence,[8] superior photostability, robust chemical inertness, and good biocompatibility[1-3]. Compared with traditional inorganic semiconductor QDs, CQDs with higher photostability and lower toxicity have shown excellent performances in bioapplications,[1-4] especially in sensors.[13-16] An effective fluorescent sensor should have high selectivity and sensitivity which is mainly related to surface functional groups of the luminous bodies and the fluorescence quantum yield (QY).[14, 17, 18] Until now, numerous methods have been utilized for the preparation of fluorescent CQDs, such as electrochemical exfoliation,[12, 13] oxidative acid treatment[19, 20] and laser ablation[21-23] of carbon materials, and hydrothermal treatment,[24-26] pyrolysis,[7, 27] microwave irradiation[28-30] and ultrasonic treatment[31] of various organic precursors. However, the QY of most CQDs is relatively low.[30, 32] To further enhance the QY, additional treatments such as surface passivation by organic molecules,[7, 33] doping with heteroatoms like nitrogen and sulfur,[16, 34-37] and size control,[23, 36] are usually needed. For all that, it is still challenging to obtain highly fluorescent CQDs on a large scale using facile approaches. To obtain highly effective CQDs-based sensors, it is very necessary to develop novel CQDs with high QY and rich surface functional groups.[38]

Hg^{2+}, one of the most hazardous and toxic cations in the environment, can accumulate very easily in the human body to destroy the central nervous and endocrine systems seriously even in a very low concentration.[14, 26, 39-41] In addition, I^- is an essential trace element in the human body, and both deficiency and excess would lead to metabolic disorders, and even brain damages.[42, 43] However, sophisticated instruments and tedious methods are prerequisite for the detection of Hg^{2+} and I^- at present.[42, 44] Thus, it is an urgent demand of to develop a facile and reliable way for the efficient detection Hg^{2+} and I^-.

In this work, we prepared nitrogen-doped CQDs (N-CQDs) with strong blue fluorescence and high QY of 66.8% by a facile one-pot hydrothermal approach using ammonium citrate and

[a] Beijing Key Laboratory of Bioprocess, College of Biology Science and Technology, Beijing University of Chemical Technology, Beijing, 100029, P. R. China.
[b] Key Laboratory of Photochemical Conversion and Optoelectronic Materials, Technical Institute of Physics and Chemistry, Chinese Academy of Sciences, Beijing, 100190, P. R. China. E-mail: tierui@mail.ipc.ac.cn; Fax: +86 10 62554670; Tel: +86 10 82543428
[c] University of Chinese Academy of Sciences, Beijing, 100049, P. R. China
‡ They make equal contributions to this study.

†Electronic Supplementary Information (ESI) available: The size distribution of N-CQDs, QY measurements, UV-Vis absorption spectra and fluorescence lifetime measurements during Hg^{2+} and I^- detections. See DOI:10.1039/b000000x

ethylenediamine as carbon and nitrogen sources. The composition, microstructures, UV-Vis absorption, and fluorescence performances of N-CQDs were well characterized. Subsequently, these as-synthesized N-CQDs as effective fluorescence probes were investigated for sensitive and selective detection of hazardous and toxic Hg^{2+} and I^-. Finally, a possible fluorescence detection mechanism of N-CQDs was put forward based on UV-Vis absorption and fluorescence decay measurements.

Experimental

Materials

Ammonium citrate, ethylenediamine, dichloromethane, methanol, ethanol, silica gel, filter membrane (0.22 μm) and kinds of metal salts, $NaNO_3$, KNO_3, $Ca(NO_3)_2$, $Mg(NO_3)_2$, $Ba(NO_3)_2$, $Al(NO_3)_3$, $Zn(NO_3)_2$, $Cu(NO_3)_2$, $FeSO_4$, $FeCl_2$, $Fe(NO_3)_3$, $Ni(NO_3)_2$, $Co(NO_3)_2$, $Mn(NO_3)_2$, $Pb(NO_3)_2$, $AgNO_3$, $Cr(NO_3)_3$, $Cd(NO_3)_2$, $Hg(ClO_4)_2$, $(CH_3COO)_2Hg$, CH_3COONa, KI, NaBr, NaCl, KF, K_2CO_3, Na_2SO_4, K_2HPO_4, KH_2PO_4, and K_3PO_4 were purchased from Beijing Chemical Reagent Plant (Beijing, China). All the above chemicals were of analytical grade and used directly.

Synthesis of N-CQDs

N-CQDs were prepared by a hydrothermal method. Ammonium citrate (8 mmol) and ethylenediamine (2 mL) were dissolved in water (10 mL). Then the solution was transferred to a Teflon-lined autoclave (50 mL) and heated at 200 ºC for 5 h. The color of the solution turned into orange-red. The collected product was dispersed in ethanol and centrifuged at 12000 rpm for 10 min. The concentrated supernatant was purified by silica gel column chromatography using methanol and dichloromethane as eluent. Finally, N-CQDs were obtained by a membrane-filter separation process.

Characterization

Transmission electron microscopic (TEM) and high resolution TEM (HRTEM) images were obtained on a JEOL-2100F microscope with an accelerating voltage of 200 kV. Fourier transform infrared (FT-IR) spectra were collected on an Excalibur 3100 spectrophotometer with a resolution of 4 cm^{-1}. X-ray photoelectron spectroscopic (XPS) measurements were performed on a Thermo Scientific ESCALab 250Xi using 200 W monochromatic Al Kα radiation. Elemental analysis was performed on a Vario EL Ⅲ analyzer. Fluorescence emission spectra measurements were carried out on a Hitachi F4600 fluorescence spectrometer. UV-Vis absorption spectra were recorded on a Hitachi U-3900 spectrophotometer. Time-resolved fluorescence decay was measured by time-correlated-single photon counting (Edinburgh Instruments, FLS-920).

Selective detection of metal cations

To investigate the interference of metal cations, many different kinds of metal cations were chosen for the detection as follows: $NaNO_3$, KNO_3, $Ca(NO_3)_2$, $Mg(NO_3)_2$, $Ba(NO_3)_2$, $Al(NO_3)_3$, $Zn(NO_3)_2$, $Cu(NO_3)_2$, $FeSO_4$, $FeCl_2$, $Fe(NO_3)_3$, $Ni(NO_3)_2$, $Co(NO_3)_2$, $Mn(NO_3)_2$, $Pb(NO_3)_2$, $AgNO_3$, $Cr(NO_3)_3$, $Cd(NO_3)_2$, $Hg(ClO_4)_2$, and $(CH_3COO)_2Hg$. Aqueous solutions of these metal salts (50.5 μM) were all freshly prepared. Typically, one aqueous solution of metal salt (50.5 μM, 1980 μL) was mixed with a dispersion of N-CQDs (0.55 mg/mL, 20μL). After the mixture was equilibrated for 10 min with stirring, the fluorescence measurement was performed.

Fluorescence detection of Hg^{2+}

$Hg(ClO_4)_2$ aqueous solution (1980 μL) with certain concentrations was first mixed with a dispersion of N-CQDs (0.55 mg/mL, 20 μL). Then the fluorescence measurement was carried out after the mixed solution was equilibrated for 10 min with stirring.

Selective detection of anions

$Hg(ClO_4)_2$ aqueous solution (30.6 μM, 1960 μL) was first mixed with a dispersion of N-CQDs (0.55 mg/mL, 20 μL) and stirred for 10 min (named N-CQDs-Hg^{2+} system). Then an aqueous solution of anions (5 mM, 20 μL) was added. Those anions included I^-, NO_3^-, PO_4^{3-}, HPO_4^{2-}, $H_2PO_4^-$, Cl^-, Br^-, SO_4^{2-}, CO_3^{2-}, F^-, and CH_3COO^-. After the mixture was equilibrated for 20 min with stirring, the fluorescence measurement was performed.

Fluorescence detection of I^-

$Hg(ClO_4)_2$ aqueous solution (30.6 μM, 1960 μL) was first mixed with a dispersion of N-CQDs (0.55 mg/mL, 20 μL) for 10 min. After different concentrations of I^- (20μL) were added and equilibrated for 20 min, the fluorescence measurements were carried out.

Results and discussion

In order to investigate the morphology of N-CQDs, TEM and HRTEM measurements were carried out. As shown in Fig. 1, N-CQDs are spherical-like with an average size of ~4.8 nm (Fig. S1). The typical lattice spacing of 0.340 nm indicates a graphitic structure of the as-obtained N-CQDs.[1, 3, 45]

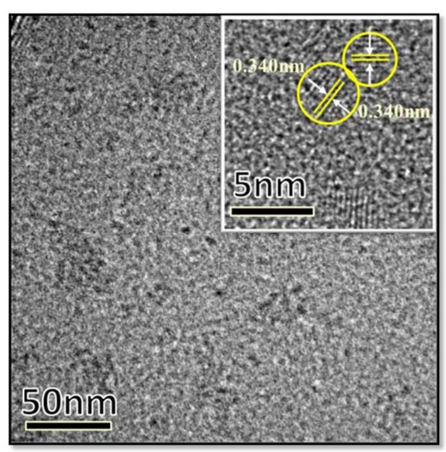

Fig. 1 TEM and HRTEM images (inset) of N-CQDs.

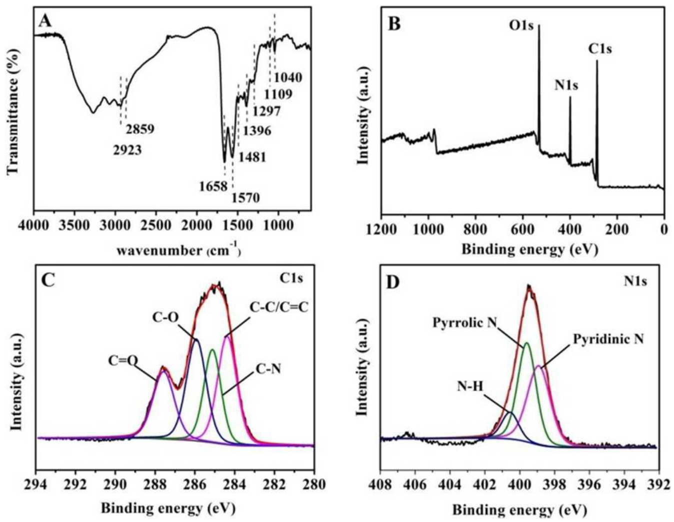

Fig. 2 Microstructure analysis of N-CQDs. FT-IR spectrum (A); Full-scale XPS spectrum (B); High resolution XPS spectra of C 1s (C) and N1s (D).

The chemical composition of N-CQDs was studied by elemental analysis and FT-IR measurements (Table S1, Fig. 2A). The characteristic absorption peaks between 3100 and 3500 cm^{-1} are assigned to the stretching vibration of $-NH_2$ and -OH.[28] The peaks at 2923 cm^{-1} and 2859 cm^{-1} are ascribed to the stretching vibrations of -C-H.[11] The typical peaks at 1570 cm^{-1} and 1658 cm^{-1} are associated with the bending vibrations of -C=O-NH-.[46] The peak at 1481 cm^{-1} is related to the stretch band of C-N (amine III), and the peaks at 1396 cm^{-1} and 1040 cm^{-1} are ascribed to the vibration of C-O.[1, 46] The above results indicate that N-CQDs have rich functional groups.

In order to gain further structural insights, XPS measurements were performed. The survey XPS spectrum (Fig. 2B) indicates the existence of three elements C, N, O in N-CQDs, which is consistent with the result of elemental analysis. The typical peaks at 284.4 eV, 285.1 eV, 286.0 eV, and 287.6 eV in the deconvoluted C1s XPS spectrum (Fig. 2C) are attributed to the graphitic (C=C, C-C), C-N, C-O and C=O, respectively.[30, 47] The typical peaks at 389.9 eV, 399.6 eV and 400.6 eV in the N1s XPS spectrum (Fig. 2D) reveal three different types of nitride: pyridinic type, pyrrolic type, and N-H.[25, 26, 30, 48] The XPS analysis is well consistent with the above FT-IR results.

The optical properties of N-CQDs were investigated by UV-Vis absorption and fluorescence spectrophotometer. It can be clearly seen in Fig. 3 that N-CQDs show two strong absorption peaks centered at 240 and 350 nm. According to previous studies, the absorption peak at 240 nm can be ascribed to π-π* transition of C=C bond, while the absorption peak at 350 nm is attributed to n-π* transition of C=O bond.[3, 16, 32, 46, 49] When excited at 360 nm, N-CQDs show a very strong emission peak centered at 445 nm (Fig. 3). Moreover, the emission peaks of N-CQDs almost keep still at 445 nm with the excitation wavelengths increasing from 280 to 400 nm (Fig. S2). The excitation-independent photoluminescence behavior could be due to few surface defects and narrow size distribution of N-CQDs.[32, 46] Notably, the strong blue fluorescence of N-CQDs excited by a 6 W hand-held UV lamp (365 nm) can be observed clearly by naked eyes (inset in Fig. 3A). The QY of N-CQDs was determined to be as high as 66.8% with quinine sulfate as a reference (Fig. S3).[1] Besides, the as-obtained N-CQDs can be well dispersed in water and polar solvents without any further surface modification. Importantly, the emission of N-CQDs is highly stable in a wide pH range from 4.0 to 10.0 (Fig. 3B). All the above advantages of as-synthesized N-CQDs indicate their great potential as highly effective fluorescence probes.

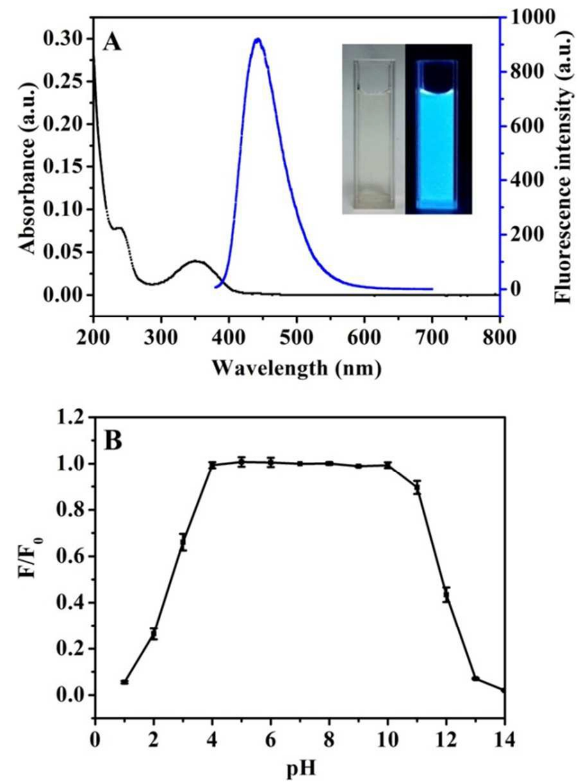

Fig. 3 UV-Vis absorption and fluorescence spectra of N-CQDs in aqueous solution (A); Digital photographs of N-CQDs without (left) and with (right) the irradiation of UV light (inset in A); The fluorescence intensity of N-CQDs in the solution dependent on different pH (B). The error bars represent the standard deviation of three parallel measurements.

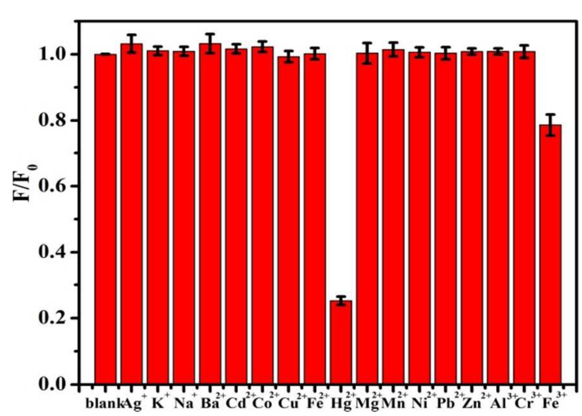

Fig. 4 Fluorescence changes of N-CQDs in the presence of different metal ions ($C_{N\text{-}CQDs}$ = 5.5 mg/L, $C_{metal\ ions}$ = 50 μM). F_0 and F represent the fluorescence intensity of N-CQDs before and after the addition of metal ions, respectively.

To demonstrate effective detection performances of N-CQDs fluorescence probes, the selective detection of metal ions was first investigated. As shown in Fig. 4, the fluorescence of N-CQDs remains nearly unchanged for 16 kinds of metal ions except for a serious fluorescence quenching by Hg^{2+}. It reveals that N-CQDs can be used for highly selective detection of Hg^{2+}, which could be due to the very strong interactions between Hg^{2+} and some surface functional groups of N-CQDs.[14]

Further, the sensitivity of the Hg^{2+} detection was explored in Fig. 5. With the concentration of Hg^{2+} increasing from 10 nM to 50 μM, the fluorescence intensity of N-CQDs at 445 nm decreases gradually. Furthermore, the fluorescence quenching level (F/F_0) is proportional to the Hg^{2+} concentrations from 10 nM to 20 μM. The detection limit was calculated to be 8.6 nM (1.72 ppb) based on the equation 3δ/m (δ is the standard deviation and m is the slope of the linear fit), which is lower than the maximum contamination level of Hg^{2+} in drinking water permitted by World Health Organization (6 ppb) and meets the limit set by the U.S. Environmental Protection Agency (2 ppb).[14, 26, 41, 50, 51] The above results demonstrate that N-CQDs can be utilized as effective fluorescence turn-off sensors for highly selective and sensitive detection of Hg^{2+}.

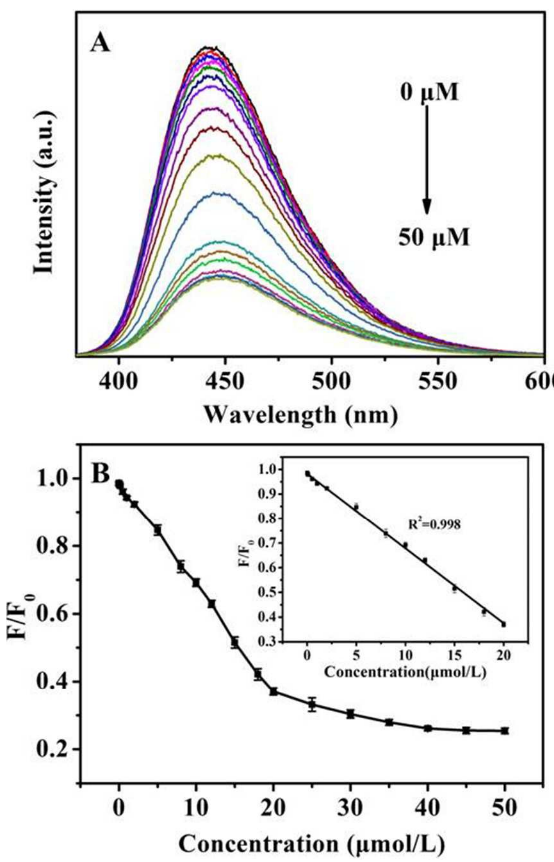

Fig. 5 Fluorescence of N-CQDs quenched by Hg^{2+} with various concentrations (from top to bottom: 0, 0.01, 0.05, 0.5, 1, 2, 5, 8, 10, 12, 15, 18, 20, 25, 30, 35, 40, 45, 50 μM) (A); Relative fluorescence intensity of N-CQDs versus the concentration of Hg^{2+} (B) (F and F_0 refer the fluorescence intensity of N-CQDs at 445 nm with and without Hg^{2+}, respectively, $C_{N\text{-}CQDs}$ = 5.5 mg/L, λ_{ex} = 360 nm).

Interestingly, the fluorescence of N-CQDs quenched by Hg^{2+} (N-CQDs-Hg^{2+}) can be easily recovered by selected anions. As shown in Fig. 6, after 11 kinds of anions are added into the N-CQDs-Hg^{2+} system, no significant fluorescence changes are observed except that 79% fluorescence is recovered with the addition of I^-, which indicates a high selectivity for I^- with the N-CQDs-Hg^{2+} system.

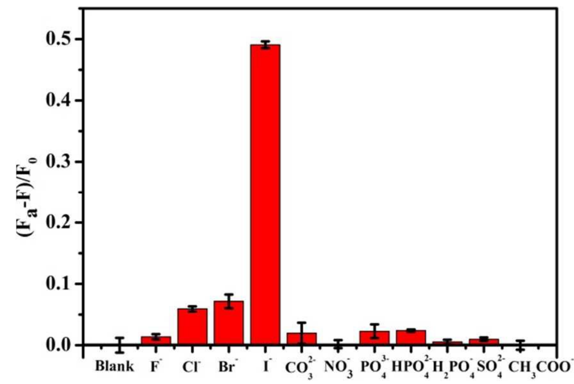

Fig. 6 Fluorescence response of the N-CQDs-Hg^{2+} system ($C_{N\text{-}CQDs}$ = 5.5 mg/L, $C_{Hg^{2+}}$ = 30 μM, λ_{ex} = 360 nm) in the presence of 11 kinds of anions (C_{anion} = 50 μM).

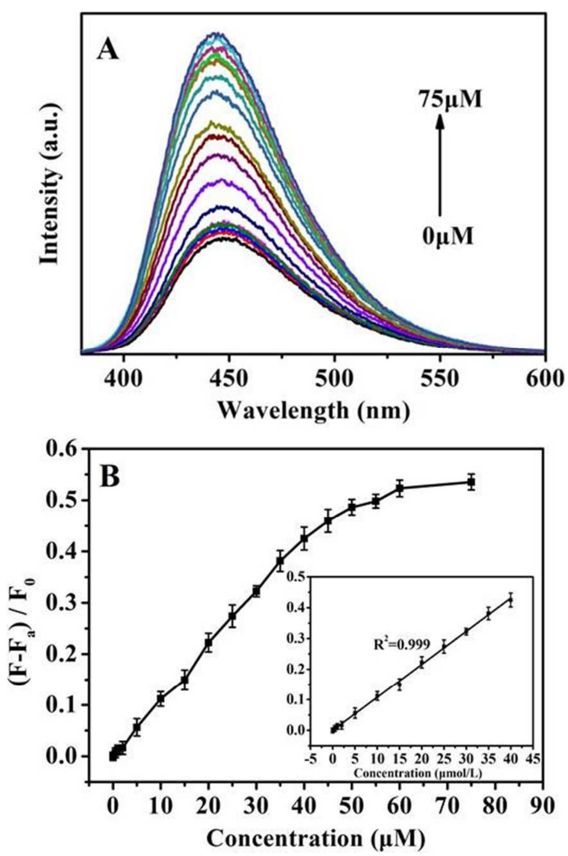

Fig. 7 Fluorescence of the N-CQDs-Hg^{2+} system dependent on different concentrations of I^- (from bottom to top: 0, 0.5, 1, 2, 5, 10, 15, 20, 25, 30, 35, 40, 45, 50, 55, 60, 75 μM) (A); Relative fluorescence intensity of the N-CQDs-Hg^{2+} system versus the concentration of I^- (B) (F_a/F_0 and F/F_0 correspond to the fluorescence intensity at 445 nm without and with I^- in the N-CQDs/Hg^{2+} system, $C_{N\text{-}CQDs}$ = 5.5 mg/L, $C_{Hg^{2+}}$ = 30 μM, λ_{ex} = 360 nm).

As shown in Fig. 7A, the fluorescence of N-CQDs-Hg^{2+} recovers gradually with the addition of I^-. And the extent of fluorescent intensity recovery ($(F-F_a)/F_0$) is almost proportional to the concentration of I^- ranging from 0.5 μM to 40 μM (63.5 to 5080 μg/L, Fig. 7B) with a detection limit of 0.354 μM (45.0 μg/L), which makes the N-CQDs-Hg^{2+} system very promising to detect I^- in human urine (100-200 μg/L).[42] These results demonstrate that N-CQDs can be utilized for the selective and sensitive detection of both Hg^{2+} and I^- through the fluorescence quenching and recovery processes, respectively.

For a better understanding on the fluorescence quenching and recovery process of N-CQDs, UV-Vis absorption and fluorescence decay measurements were performed.[52-54] It can be clearly seen in Fig. S4 that the typical absorption peak of N-CQDs at 350 nm red-shifts to 370 nm after the addition of Hg^{2+}, suggesting that Hg^{2+} could interact with N-CQDs to affect the charge transfer process on N-CQDs.[53] After adding I^- into the N-CQDs-Hg^{2+} system, the absorption peak moves back to 350 nm again, which implies that Hg^{2+} could take off from N-CQDs due to the formation of HgI_2.[14]

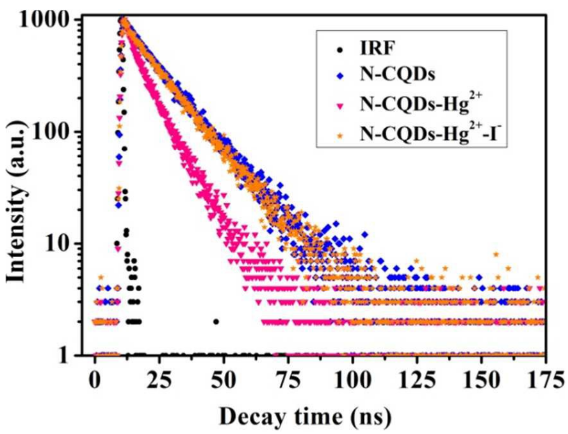

Fig. 8 Fluorescence decay traces of N-CQDs (5.5 mg/L) (blue-square), N-CQDs in the presence of Hg^{2+} (30 μM) as turn-off sensor (pink-rectangular), and N-CQDs-Hg^{2+} after adding I^- (50μM) ($C_{N\text{-}CQDs}$ = 5.5 mg/L, C_{Hg}^{2+} = 30 μM) as turn-on sensor (orange-star). λ_{ex} = 340 nm, λ_{em} = 445 nm. IRF is the instrument response function.

The charge transfer between N-CQDs and ions (Hg^{2+} and I^-) during the fluorescence quenching and recovery processes were further investigated by fluorescence decay measurements. The fluorescent lifetime of N-CQDs consists of two parts (Table S2). The short lifetime (τ_1 = 2.91 ns, 4.08%) can be related to the intrinsic states of N-CQDs, and the long lifetime (τ_2 = 15.30 ns, 95.92%) can be associated with the surface states of N-CQDs (Fig. 8, blue-square).[53, 55] After adding Hg^{2+} into N-CQDs, the average lifetime of N-CQDs decreases from 14.79 ns to 8.77 ns (Fig. 8, pink-rectangular) accompanied with remarkable fluorescence quenching (Fig. 5), implying the fast charge transfer between N-CQDs and Hg^{2+}.[26, 54, 56] Additionally, the percentage of τ_2 decreases to 81.31%, indicating that the surface states of N-CQDs are affected by Hg^{2+}.[53, 55] After adding I^- into the N-CQDs-Hg^{2+} system, the average lifetime of N-CQDs recovers to 14.43 ns and the percentage of τ_2 restores to 97.13% (Fig. 8, orange-star), approaching to the original values. This indicates that the charge transfer between N-CQDs and Hg^{2+} is interrupted due probably to the formation of HgI_2.

Based on the above results, it can be concluded that the fluorescence quenching of N-CQDs during Hg^{2+} detection is caused by the charge transfer between N-CQDs and Hg^{2+}, and the fluorescence recovery of N-CQDs-Hg^{2+} during I^- detection is due to the formation of HgI_2 (Scheme 1).

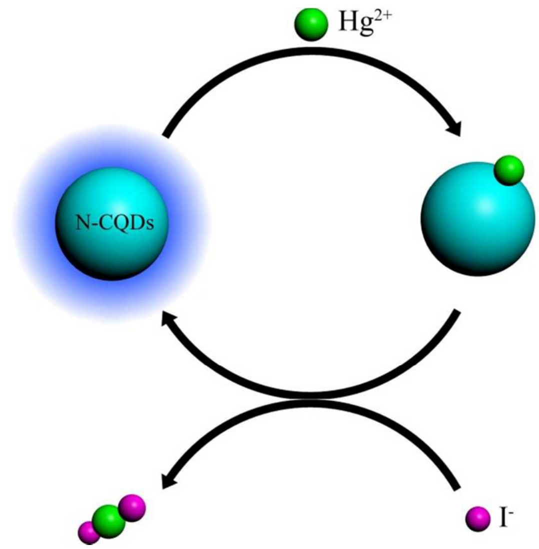

Scheme 1 Schematic illustration of the fluorescence quenching and recovery processes of N-CQDs during Hg^{2+} and I^- detections.

Conclusion

In conclusion, we have successfully synthesized one kind of novel N-CQDs by a one-pot hydrothermal approach in which ammonium citrate and ethylenediamine were used as carbon and nitrogen sources. The as-prepared N-CQDs exhibit very strong blue fluorescence with a high QY of 66.8%. The fluorescence emission is independent of the excitation wavelength. Moreover, the fluorescence emission is very stable in a wide pH range from 4.0 to 10.0. Additionally, these N-CQDs can be well dispersed in water and other polar solvents. These N-CQDs show highly selective and sensitive detection of Hg^{2+} via a fluorescence quenching process with a detection limit of 8.6 nM (1.72 ppb). Further, the quenched N-CQDs-Hg^{2+} shows highly selective and sensitive detection of I^- via a fluorescence recovery process with a detection limit of 0.354 μM (45.0 μg/L). UV-Vis absorption and fluorescence decay measurements suggest that the fluorescence quenching and recovery processes during Hg^{2+} and I^- detections are closely related to the charge transfer between Hg^{2+} and N-CQDs. Therefore, N-CQDs are very promising for future practical detections of hazardous and toxic ions.

Acknowledgements

We are very grateful for the support from the Ministry of Science and Technology of China (2013CB834505, 2014CB239402), the Key Research Program of the Chinese Academy of Sciences, the National Natural Science Foundation of China (21401206, 51322213, 21301183, 51172245, 91127005, 21401207), the Beijing Natural Science Foundation (2152033, 2122054, 2154058), the Ten Thousand Talents Plan and the 100 Talents Program of the Chinese Academy of Sciences.

Notes and references

1. S. Zhu, Q. Meng, L. Wang, J. Zhang, Y. Song, H. Jin, K. Zhang, H. Sun, H. Wang and B. Yang, *Angew. Chem., Int. Ed.*, 2013, **52**, 3953-3957.
2. H. Ding, L.-W. Cheng, Y.-Y. Ma, J.-L. Kong and H.-M. Xiong, *New J. Chem.*, 2013, **37**, 2515-2520.
3. J. Gong, X. An and X. Yan, *New J. Chem.*, 2014, **38**, 1376-1379.
4. Y. F. Huang, X. Zhou, R. Zhou, H. Zhang, K. B. Kang, M. Zhao, Y. Peng, Q. Wang, H. L. Zhang and W. Y. Qiu, *Chemistry*, 2014, **20**, 5640-5648.
5. P. Juzenas, A. Kleinauskas, P. George Luo and Y.-P. Sun, *Appl. Phys. Lett.*, 2013, **103**, 063701.
6. S. Pandey, M. Thakur, A. Mewada, D. Anjarlekar, N. Mishra and M. Sharon, *J. Mater. Chem. B,* 2013, **1**, 4972-4982.
7. C. Lai, Y. Hsiao, Y. Peng and P. Chou, *J. Mater. Chem.*, 2012, **22**, 14403-14409.
8. H. Li, X. He, Z. Kang, H. Huang, Y. Liu, J. Liu, S. Lian, C. H. Tsang, X. Yang and S. T. Lee, *Angew. Chem., Int. Ed.*, 2010, **49**, 4430-4434.
9. H. Li, R. Liu, S. Lian, Y. Liu, H. Huang and Z. Kang, *Nanoscale*, 2013, **5**, 3289-3297.
10. Y. Li, B.-P. Zhang, J.-X. Zhao, Z.-H. Ge, X.-K. Zhao and L. Zou, *Appl. Surf. Sci.*, 2013, **279**, 367-373.
11. V. Gupta, N. Chaudhary, R. Srivastava, G. D. Sharma, R. Bhardwaj and S. Chand, *J. Am. Chem.Soc.*, 2011, **133**, 9960-9963.
12. Y. Li, Y. Hu, Y. Zhao, G. Shi, L. Deng, Y. Hou and L. Qu, *Adv. Mater.*, 2011, **23**, 776-780.
13. A. Ananthanarayanan, X. Wang, P. Routh, B. Sana, S. Lim, D.-H. Kim, K.-H. Lim, J. Li and P. Chen, *Adv. Funct. Mater.*, 2014, **24**, 3021-3026.
14. S. Barman and M. Sadhukhan, *J. Mater. Chem.*, 2012, **22**, 21832-21837.
15. Y. Dong, R. Wang, G. Li, C. Chen, Y. Chi and G. Chen, *Anal. Chem.*, 2012, **84**, 6220-6224.
16. S. Li, Y. Li, J. Cao, J. Zhu, L. Fan and X. Li, *Anal. Chem.*, 2014, **86**, 10201-10207.
17. H. Zheng, Q. Wang, Y. Long, H. Zhang, X. Huang and R. Zhu, *Chem. Commun.*, 2011, **47**, 10650-10652.
18. L. Bao, Z. L. Zhang, Z. Q. Tian, L. Zhang, C. Liu, Y. Lin, B. Qi and D. W. Pang, *Adv. Mater.*, 2011, **23**, 5801-5806.
19. H. Liu, T. Ye and C. Mao, *Angew. Chem., Int. Ed.*, 2007, **46**, 6473-6475.
20. R. Sekiya, Y. Uemura, H. Murakami and T. Haino, *Angew. Chem., Int. Ed.*, 2014, **53**, 5619-5623.
21. P. Atienzar, A. Primo, C. Lavorato, R. Molinari and H. Garcia, *Langmuir*, 2013, **29**, 6141-6146.
22. J. Wang, C. Wang, and S. Chen, *Angew. Chem., Int. Ed.*, 2012, **51**, 9297-9301.
23. Y. P. Sun, B. Zhou, Y. Lin, W. Wang, K. A. S. Fernando, P. Pathak, M. J. Meziani, B. A. Harruff, X. Wang, H. F. Wang, P. J. G. Luo, H. Yang, M. E. Kose, B. L. Chen, L. M. Veca, S. Y. Xie, *J. Am. Chem. Soc.* 2006, **128**, 7756-7757.
24. K. Lawrence, F. Xia, R. L. Arrowsmith, H. Ge, G. W. Nelson, J. S. Foord, M. Felipe-Sotelo, N. D. Evans, J. M. Mitchels, S. E. Flower, S. W. Botchway, D. Wolverson, G. N. Aliev, T. D. James, S. I. Pascu and F. Marken, *Langmuir*, 2014, **30**, 11746-11752.
25. S. Liu, J. Tian, L. Wang, Y. Zhang, X. Qin, Y. Luo, A. M. Asiri, A. O. Al-Youbi and X. Sun, *Adv .Mater.*, 2012, **24**, 2037-2041.
26. W. Lu, X. Qin, S. Liu, G. Chang, Y. Zhang, Y. Luo, A. M. Asiri, A. O. Al-Youbi and X. Sun, *Anal. Chem.*, 2012, **84**, 5351-5357.
27. Y. Dong, R. Wang, H. Li, J. Shao, Y. Chi, X. Lin and G. Chen, *Carbon*, 2012, **50**, 2810-2815.
28. J. Hou, J. Yan, Q. Zhao, Y. Li, H. Ding and L. Ding, *Nanoscale*, 2013, **5**, 9558-9561.
29. C. M. Luk, L. B. Tang, W. F. Zhang, S. F. Yu, K. S. Teng and S. P. Lau, *J. Mater. Chem.*, 2012, **22**, 22378-22381.
30. J. Wang, C. Cheng, Y. Huang, B. Zheng, H. Yuan, L. Bo, M.-W. Zheng, S.-Y. Yang, Y. Guo and D. Xiao, *J. Mater. Chem. C*, 2014, **2**, 5028-5035.
31. H. Li, X. He, Y. Liu, H. Huang, S. Lian, S.-T. Lee and Z. Kang, *Carbon*, 2011, **49**, 605-609.
32. Y. Dong, H. Pang, H. B. Yang, C. Guo, J. Shao, Y. Chi, C. M. Li and T. Yu, *Angew. Chem., Int. Ed.*, 2013, **52**, 7800-7804.
33. Z. Zhang, Y. Shi, Y. Pan, X. Cheng, L. Zhang, J. Chen, M.-J. Li and C. Yi, *J. Mater. Chem. B,* 2014, **2**, 5020-5027.
34. C. Wang, X. Wu, X. Li, W. Wang, L. Wang, M. Gu and Q. Li, *J. Mater. Chem. B,* 2012, **22**, 15522-15525.
35. X. Zhai, P. Zhang, C. Liu, T. Bai, W. Li, L. Dai and W. Liu, *Chem.* Commun., 2012, **48**, 7955-7957.
36. M. A. Sk, A. Ananthanarayanan, L. Huang, K. H. Lim and P. Chen, *J. Mater. Chem. C,* 2014, **2**, 6954-6960.
37. H. Ding, J. S. Wei and H. M. Xiong, *Nanoscale*, 2014, 6, 13817-13823.
38. H. Sun, N. Gao, L. Wu, J. Ren, W. Wei and X. Qu, *Chemistry*, 2013, **19**, 13362-13368.
39. B. Cao, C. Yuan, B. Liu, C. Jiang, G. Guan and M. Y. Han, *Anal. Chim. Acta*, 2013, **786**, 146-152.
40. J. Du, Y. Sun, L. Jiang, X. Cao, D. Qi, S. Yin, J. Ma, F. Y. Boey and X. Chen, *Small*, 2011, **7**, 1407-1411.
41. J. Du, L. Jiang, Q. Shao, X. Liu, R. Marks, J. Ma, and X. Chen, *Small*, 2013, **9**, 1467–1481
42. F. Du, F. Zeng, Y. Ming and S. Wu, *Microchim. Acta*, 2013, **180**, 453-460.
43. Y. Xiao, Y. Zhang, H. Huang, Y. Zhang, B. Du, F. Chen, Q. Zheng, X. He and K. Wang, *Talanta*, 2015, **131**, 678-683.
44. J. Du, B. Zhu, X. Peng and X. Chen, *Small*, 2014, **10**, 3461-3479.
45. Y. Hao, Z. Gan, J. Xu, X. Wu and P. K. Chu, *Appl. Surf. Sci.*, 2014, **311**, 490-497.
46. Z. Yang, M. Xu, Y. Liu, F. He, F. Gao, Y. Su, H. Wei and Y. Zhang, *Nanoscale*, 2014, **6**, 1890-1895.

47. Y. Fan, H. Cheng, C. Zhou, X. Xie, Y. Liu, L. Dai, J. Zhang and L. Qu, *Nanoscale*, 2012, **4**, 1776-1781.
48. S. Zhang, J. Li, M. Zeng, J. Xu, X. Wang and W. Hu, *Nanoscale*, 2014, **6**, 4157-4162.
49. W.-W. Liu, Y.-Q. Feng, X.-B. Yan, J.-T. Chen and Q.-J. Xue, *Adv. Funct. Mater.*, 2013, **23**, 4111-4122.
50. J. Liu, X. Ren, X. Meng, Z. Fang and F. Tang, *Nanoscale*, 2013, **5**, 10022-10028.
51. J. Du, B. Zhu and X. Chen, *Small*, 2013, **9**, 4104-4111.
52. L. Zhou, Y. Lin, Z. Huang, J. Ren and X. Qu, *Chem. Commun.*, 2012, **48**, 1147-1149.
53. H. Chakraborti, S. Sinha, S. Ghosh and S. K. Pal, *Mater. Lett.*, 2013, **97**, 78-80.
54. Y.-L. Zhang, L. Wang, H.-C. Zhang, Y. Liu, H.-Y. Wang, Z.-H. Kang and S.-T. Lee, *RSC Advances*, 2013, **3**, 3733-3738.
55. S. Kim, D. Hee Shin, C. Oh Kim, S. Seok Kang, J. Min Kim, S.-H. Choi, L.-H. Jin, Y.-H. Cho, S. Won Hwang and C. Sone, *Appl. Phys. Lett.*, 2012, **101**, 163103.
56. R. Liu, H. Li, W. Kong, J. Liu, Y. Liu, C. Tong, X. Zhang and Z. Kang, *Mater. Res. Bull.*, 2013, **48**, 2529-2534.

Graphical Abstract

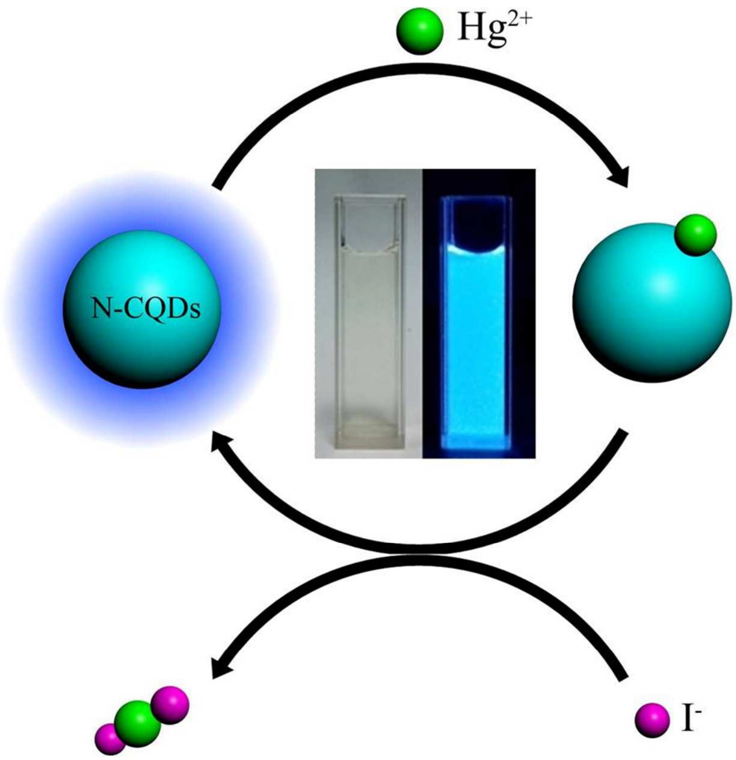

Nitrogen-doped carbon quantum dots (N-CQDs) prepared via a one-step hydrothermal reaction exhibited highly selective and sensitive detection of Hg^{2+} and I^- through flurescence quenching and recovery processes, respectively.